Parallel reaction pathways and noncovalent intermediates in thymidylate synthase revealed by experimental and computational tools

Svetlana A. Kholodar (Холодарь Светлана Алексеевна)[a,1,2], Ananda K. Ghosh[a], Katarzyna Świderek[b], Vicent Moliner[b,1], and Amnon Kohen[a]

[a]Department of Chemistry, The University of Iowa, Iowa City, IA 52242-1727; and [b]Departament de Química Física i Analítica, Universitat Jaume I, 12071 Castello, Spain

Thymidylate synthase was one of the most studied enzymes due to its critical role in molecular pathogenesis of cancer. Nevertheless, many atomistic details of its chemical mechanism remain unknown or debated, thereby imposing limits on design of novel mechanism-based anticancer therapeutics. Here, we report unprecedented isolation and characterization of a previously proposed intact noncovalent bisubstrate intermediate formed in the reaction catalyzed by thymidylate synthase. Free-energy surfaces of the bisubstrate intermediates interconversions computed with quantum mechanics/molecular mechanics (QM/MM) methods and experimental assessment of the corresponding kinetics indicate that the species is the most abundant productive intermediate along the reaction coordinate, whereas accumulation of the covalent bisubstrate species largely occurs in a parallel nonproductive pathway. Our findings not only substantiate relevance of the previously proposed noncovalent intermediate but also support potential implications of the overstabilized covalent intermediate in drug design targeting DNA biosynthesis.

thymidylate synthase | intermediate kinetics | QM/MM calculations | free-energy surfaces

Thymidylate synthase (TSase) was one of the first known anticancer drug targets due to its fundamental role in DNA biosynthesis. Currently, most successful and widely used anticancer treatments include agents specifically targeting TSase as mechanism-based inhibitors (e.g., fluoropyrimidines, such as capecitabine and tegafur). Other chemotherapeutic drugs mimic the folate substrate of this enzyme, but no drug has combined both moieties (1). Despite many therapeutic advantages, current drugs are highly toxic and lead to resistance in tumor cells. Demand for novel selective classes of TSase inhibitors fuels reexamination of its mechanistic features to establish new molecular targets.

TSase catalyzes reductive methylation of dUMP, where cosubstrate N5N10-methylenetetrahydrofolate (CH_2H_4F) consecutively donates a methylene and a hydride to form thymidylate (dTMP). The mechanism of this transformation was proposed over 20 y ago (2). While main features of this mechanism are commonly recognized, certain details are open to debate. All previous studies agree that the reaction is initiated on Michael addition of the active site thiolate (Cys146) to the C6 position of dUMP and formation of covalent ternary complex Int (Scheme 1, step 1) [note that there is a debate on whether this step occurs through a stepwise or concerted mechanism (2–7)].

However, two alternative pathways were proposed for the subsequent proton abstraction step 2. Traditional mechanism A features generation of the covalent enolate (or enol) intermediate Int-A. Indirect support for existence of Int-A is provided by model studies of the nonenzymatic proton exchange or dehalogenation at C5 of dUMP in the presence of thiols (2). In contrast, recent quantum mechanics/molecular mechanics (QM/MM) calculations predicted a much lower-energy pathway

B where the proton abstraction would occur concertedly with C6-S bond cleavage, leading to the noncovalent intermediate Int-B (6, 8). Both pathways predict conversion of Int-A or Int-B to the covalent exocyclic methylene intermediate (steps 3A and 3B), which undergoes concerted reduction and C-S bond cleavage (step 4) to result in a final product dTMP (6, 9).

As a matter of fact, despite multiple intermediates having been proposed along the reaction pathway of TSase, none of them have ever been unambiguously structurally characterized. Several studies reported detection of the intermediate covalently bound to the active site cysteine of *Lactobacillus casei* and *Cryptosporidium hominis* TSases, presumably representing Int or Int-A (10–12). However, the only structural evidence involved presence of radioactive labels originating from both of the substrates (dUMP and CH_2H_4F) in the detected covalent adducts. Studies by Anderson and coworkers (12–14) on *C. hominis* TSase indicated isolation of a noncovalent intermediate on rapid quenching with potassium hydroxide (but not on acid quenching). However, no attempt was made to characterize the structure of the detected species, and it was proposed to represent the iminium ion form of CH_2H_4F. In the work of Schultz and

Significance

Thymidylate synthase (TSase) is one of the prime anticancer targets, as it generates the sole de novo source of thymidylate, a unique precursor for DNA. Fluoropyrimidines and antifolates inhibiting TSase pathways are not only components of the most widely used therapeutic regimens but also highly toxic agents leading to acquired resistance in tumor cells. To provide fresh mechanistic insight to TSase-targeted drug design, we used a combination of experiments, kinetic modeling, and quantum mechanics/molecular mechanics (QM/MM) calculations to discover formation of unexpected noncovalent intermediates prevailing in the catalysis and overstabilized covalent species corresponding to a parallel reaction pathway. These findings challenge the traditional chemical path of this enzyme and offer drug targets.

BIOCHEMISTRY

BIOPHYSICS AND COMPUTATIONAL BIOLOGY

Scheme 1. (A) Traditional and (B) proposed mechanisms of TSase-catalyzed reaction.

coworkers (4), the existence of the covalent exocyclic methylene intermediate was indirectly supported on its trapping with β-mercaptoethanol in TSase mutants. However, no report described isolation and characterization of an intact intermediate of TSase.

In a critical test of previous QM/MM predictions (6, 8), we recently showed that chemically synthesized Int-B is indeed a chemically and kinetically competent intermediate of the reaction (15). Interestingly, inspection of the kinetics of Int-B turnover by TSase suggested that its accumulation during the natural course of the reaction would be sufficient for its detection in a rapid quench experiment. These findings encouraged us to attempt detection of Int-B transiently generated by TSase. In this work, using a rapid chemical quench technique, we showed formation of Int-B from the substrates dUMP and CH_2H_4F in the presence of *Escherichia coli* thymidylate synthase (*Ec*TSase) and characterized its kinetics. Furthermore, we utilized kinetic modeling along with QM/MM calculations to shed light on the mechanism of the bisubstrate intermediates interconversion in the active site of TSase. Our studies support that noncovalent bisubstrate intermediates dominate in the catalytic mechanism of TSase, whereas covalent bisubstrate species are formed in a parallel nonproductive pathway.

Results and Discussion

Noncovalent Intermediate of TSase Is Formed During the Natural Course of the Reaction. We performed a rapid chemical quench of the *Ec*TSase-catalyzed reaction containing [2-^{14}C]dUMP and [6-^{3}H]CH_2H_4F and found both of the labels not only in dTMP but also, in another species (Fig. 1*B*) independent of the nature of the quencher (acid or base). Note that the peak observed with UV detection at 16.6 min in Fig. 1*A* corresponds to [6-^{3}H]H_4F, which is in equilibrium with [6-^{3}H]CH_2H_4F (15). Therefore, ^{3}H signal at 18–20 min in Fig. 1*B* results from the overlap of the signal corresponding to [6-^{3}H]H_4F and the double-labeled species. Due to potential ambiguity of double-labeling experiment caused by the interference of ^{3}H signals of the folate derivatives generated nonenzymatically from [6-^{3}H]CH_2H_4F, we performed additional experiments to gain certainty in the structure of the detected intermediate. A peak arising from double-labeled species was also observed with UV detection at 18.2 min (Fig. 1*A*). Using the standard synthetic Int-B, we showed that retention time, UV spectrum (Fig. 1*A*, *Inset*), and mass [high-resolution mass spectrometry *m/z* (electrospray ionization) [M-H$^+$]: observed

764.2050, standard 764.2047, calculated 764.2041] of the unknown species are in excellent agreement with those of Int-B.

Kinetics of Noncovalent and Covalent Intermediate(s) Formation in the TSase-Catalyzed Reaction Implies Parallel Reaction Pathways. To gain additional support for kinetic competence of the detected intermediate, we followed the time course of its transient formation as well as dUMP consumption and dTMP generation (Fig. 2, blue, pink, and green dots, respectively) on turnover of [2-^{14}C]dUMP in the presence of unlabeled CH_2H_4F and rapid quenching of the reaction mixture with NaOH (0.33 M final; base quench). Under these conditions, maximum accumulation of intermediate reached ca. 34% of the total radioactivity, and no radioactivity was associated with protein, suggesting that covalently bound intermediates either are not accumulated to a detectable extent or are artificially released from the active site under basic conditions. In contrast, when HCl (0.33 M final; acid quench) was used as a quencher, despite that noncovalent intermediate was observed in the solution, a significant amount of either covalently bound or coprecipitated ^{14}C label was found in the protein pellet, even for the reactions quenched after completion. Note that nucleotides are known to combine covalently with TSase even in the absence of any folates, and these covalent complexes are stable under acid quench conditions (10).
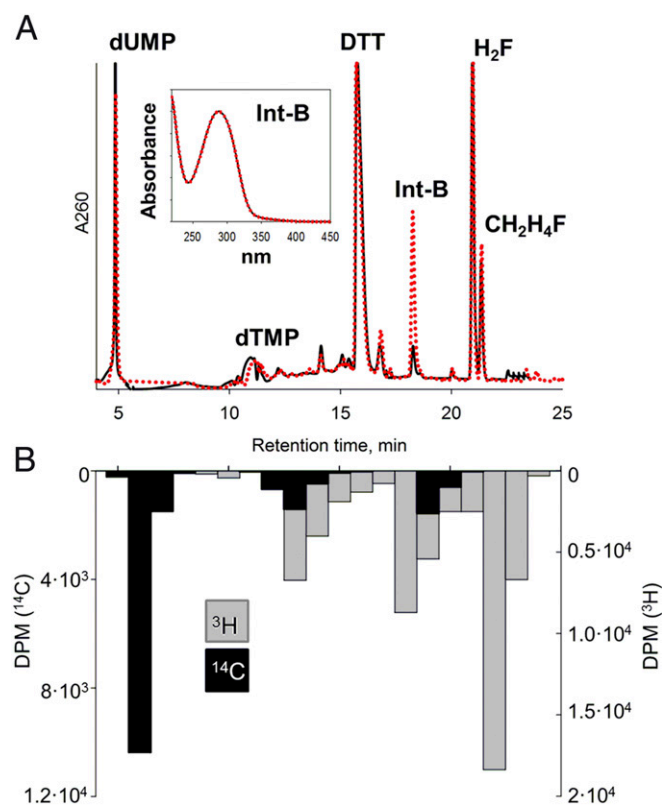
Fig. 1. (A) Chromatogram at 260 nm of the *Ec*TSase-catalyzed reaction mixture quenched after 100 ms with hydrochloric acid (solid black) superimposed with the same reaction mixture coinjected with standard synthetic Int-B (dotted red). (*Inset*) The UV spectrum of the peak at 18.2 min (solid black) superimposed with the UV spectrum of standard Int-B (dotted red). Reaction conditions: 50 μM *Ec*TSase (dimer), 100 μM dUMP, 100 μM CH_2H_4F, 100 mM Tris·HCl, pH 7.5, 25 mM DTT, and 7 mM HCHO. (B) HPLC radiogram of the *Ec*TSase-catalyzed reaction mixture quenched after 100 ms with hydrochloric acid. Reaction conditions: 50 μM *Ec*TSase (dimer), 100 μM [2-^{14}C]dUMP, 200 μM [6-^{3}H]CH_2H_4F, 100 mM Tris·HCl, pH 7.5, 25 mM DTT, and 7 mM HCHO. Note the presence of both ^{14}C and ^{3}H labels in the peak corresponding to Int-B (retention time: 18–20 min). DPM, disintegrations per minute.
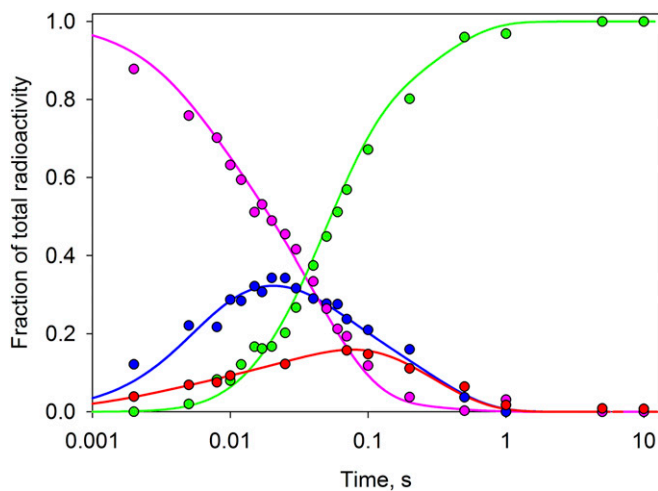
Fig. 2. Single-turnover kinetics of the *Ec*TSase-catalyzed reaction measured by rapid chemical quench with NaOH: time course for [2-^{14}C]dUMP (pink) consumption, dTMP (green) formation, and Int-B (blue) transient generation. Reaction conditions: 100 μM *Ec*TSase (dimer), 80 μM [2-^{14}C]dUMP, 200 μM CH$_2$H$_4$F, 100 mM Tris·HCl, pH 7.5, 50 mM MgCl$_2$, 25 mM DTT, and 7 mM HCHO at 25 °C. Single-turnover kinetics of the *Ec*TSase-catalyzed reaction measure by rapid chemical quench with HCl: time course for [3′,5′,7,9-^{3}H]CH$_2$H$_4$F derived covalently bound to the enzyme intermediates (red). Reaction conditions: 150 μM *Ec*TSase (dimer), 400 μM dUMP, 80 μM [3′,5′,7,9-^{3}H]CH$_2$H$_4$F, 100 mM Tris·HCl, pH 7.5, 50 mM MgCl$_2$, 25 mM DTT, and 7 mM HCHO at 25 °C. Dots represent experimental data points, and lines are the global fit of the entire dataset (including additional steady-state and presteady-state kinetics data provided in *SI Appendix*) to *SI Appendix*, Scheme S1 (kinetic model based on the QM/MM proposed molecular mechanism outlined in Fig. 3*A*) using KinTek Explorer. Each curve was reproduced in at least two independent experiments.

Therefore, accurate measurement and interpretation of the kinetics of the noncovalent reaction components recovered under conditions of the acid quench are compromised when radioactive label is in the nucleotide. However, using radiolabeled CH$_2$H$_4$F would allow for avoiding complexity associated with covalent retention of nucleotides. However, inevitable equilibrium between CH$_2$H$_4$F and H$_4$F and the unstable nature of the folates lacking substitution at the position N5 preclude quantitative assessment of the noncovalent reaction components, as it is also

discussed in the previous section. Since the focus of this study was to investigate mechanistic details of formation and interconversion of the bisubstrate intermediates of the reaction, we chose to use base quench conditions and [2-^{14}C]dUMP for accurate examination of the kinetics of the ^{14}C-labeled substrates, products, and bisubstrate intermediates (covalent and noncovalent). All of these species are quantitatively released from TSase and are stable in the base. Furthermore, we exploited the ability of the acid quench to preserve covalent interactions between TSase and its intermediates to quantify the contribution of covalent bisubstrate intermediates under the base quench conditions.

To avoid ambiguity of the signal originating from multiple covalent enzyme complexes derived from radiolabeled nucleotide as discussed above (10), we examined the time course of covalently bound radiolabel originating from the folate. Using [3′,5′,7,9-^{3}H]CH$_2$H$_4$F and unlabeled dUMP, we followed accumulation of the radioactivity covalently bound to protein on rapid quenching of the reaction mixture with HCl (0.33 M final) (Fig. 2, red dots). Any noncovalently bound ligands were removed on denaturation of the protein with 2% SDS at pH 7.5 and spin filtration through a 10-kDa cutoff membrane. Although the exact structure of the covalently bound adduct had not been determined in this work, folate can only be covalently bound to the TSase active site if it is a part of ternary covalent complex Int, Int-A, and/or their corresponding protonated forms. As follows from Fig. 2, covalently bound intermediate(s) accounts only for a fraction of the total pool of Int-B detected on quenching with base. This observation supports that the total Int-B is a sum of Int-B generated by TSase and Int-B artificially generated from covalent intermediate(s) in the presence of base. Surprisingly, formation and decay of the covalent intermediate(s) were considerably slower (ca. threefold) than formation and decay of total noncovalent Int-B observed in the base quench. Therefore, we concluded that covalent intermediates are largely represented by the species forming parallel to the major pathway leading to the product dTMP. In agreement with this interpretation, previous studies by Hardy and coworkers (16, 17) suggested that covalent ternary complex Int-A is especially vulnerable to overstabilization by *Ec*TSase, and it is likely a nonproductive fully reversible complex that branches from the major reaction pathway.
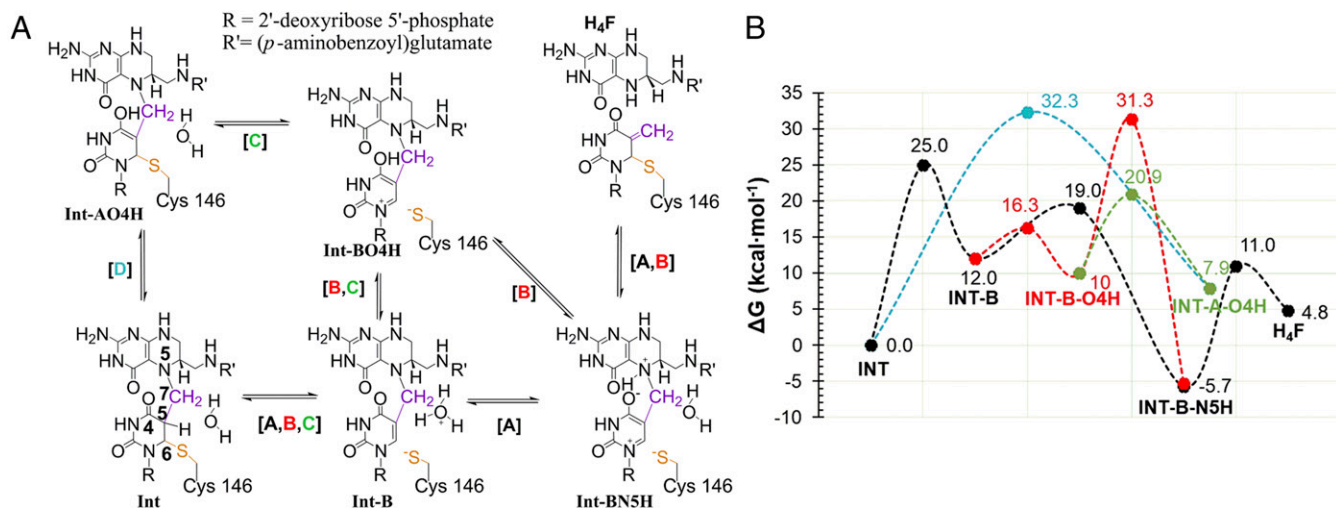
Fig. 3. QM/MM proposed molecular mechanism of the bisubstrate intermediates interconversion in the active site of TSase (*A*) and the corresponding free-energy profile (*B*).

Agreement Between QM/MM Calculations and Experimental Data Supports Existence of Parallel Pathways and Prevalence of Noncovalent Intermediates in TSase Catalytic Mechanism. To get a deeper insight into the mechanism complementing and supporting the kinetic studies, hybrid QM/MM calculations have been carried out with the QM subset of atoms described at the density functional theory (DFT) level with the B3LYP (Becke, 3-parameter, Lee-Yang-Parr) functional and the rest of the protein and solvating water molecules treated with OPLS-AA (optimized potential for liquid simulations–all atom) and TIP3P (transferable intermolecular potential–3 point) classical force fields, respectively (*SI Appendix* has details). The obtained free-energy landscape of the reaction suggests that Int-B partitions between its N5- and O4-protonated forms (Fig. 3). However, the H$_4$F and exocyclic methylene intermediate products can be reached only from a direct C7-N5^{FOL} cleavage from Int-B-N5H as previously proposed (6). In contrast, productive decomposition of Int-BO4H must proceed either through reversal to Int-B followed by N5 protonation or through the significantly higher-energy direct formation of Int-B-N5H. Interestingly, calculations suggest that an alternative fate of IntB-O4H involves restoration of the C6-S bond, resulting in covalent species Int-AO4H. The latter is effectively a dead-end species, as no forward pathway toward product formation was found. Notably, this prediction agrees with the experimentally suggested conclusion that the covalent bisubstrate intermediate is predominantly forming in a parallel nonproductive reaction pathway.

Directed by the molecular mechanism outlined in Fig. 3*A* and using KinTek Explorer, we globally fit the entire set of the rapid quench data and previously obtained steady-state and presteady-state kinetics of the reaction [including steady-state kinetics of externally added Int-B turnover (15)] and found a solution consistent with the proposed pathway (Fig. 2*A*, global fit; *SI Appendix* has details). Since it was only possible to monitor a total pool of bisubstrate intermediates and its subset corresponding to covalent species, the kinetics of each individual intermediate was simulated and represents one of the possible solutions, which globally fits to experimental data points. However, we were able to achieve a reasonably good agreement between QM/MM calculations and the global fit to experimental data combined with the simulation. First, both QM/MM calculations and the KinTek simulation predict that the total pool of bisubstrate intermediates is predominantly represented by noncovalent species, where the Int-B-N5H form is likely the most stable intermediate. Second, partitioning of Int-B between two parallel pathways happens with comparable probabilities. Third, formation of "dead-end" covalent intermediate Int-A-O4H on restoration of C6-S bond to Int-B-O4H is a thermodynamically favorable process that competes with the reversal of Int-B-O4H to Int-B and therefore, the productive reaction path.

In summary, this work provides several important milestones to the current knowledge of the catalytic mechanism of TSase. Specifically, we report isolation and characterization of the intact noncovalent bisubstrate intermediate of the reaction. Investigation of the interconversions of this intermediate through the combination of QM/MM methods, experiments, and kinetic modeling reveals that this noncovalent species is indeed the major productive intermediate along the reaction pathway, whereas the covalent species forms in a parallel nonproductive pathway. Both computational and experimental results reinforce each other in their description of a branched path mechanism, where a covalent bisubstrate species is implicated as an overstabilized intermediate of the reaction. The latter finding could be a useful direction for TSase-targeted drug discovery, as it unveils a weak spot in the catalytic mechanism, which could be exploited in efforts to inhibit the enzyme.

Materials and Methods

Detailed information on the *Ec*TSase expression and purification, labeled substrate synthesis, enzymatic assays, rapid chemical quench procedures, HPLC analysis, data fitting and kinetic modeling with KinTek Explorer, computational methods, and QM/MM free-energy surfaces is provided in *SI Appendix*.

1. Wilson PM, Danenberg PV, Johnston PG, Lenz HJ, Ladner RD (2014) Standing the test of time: Targeting thymidylate biosynthesis in cancer therapy. *Nat Rev Clin Oncol* 11:282–298.
2. Carreras CW, Santi DV (1995) The catalytic mechanism and structure of thymidylate synthase. *Annu Rev Biochem* 64:721–762.
3. Rode W, Leś A (1996) Molecular mechanism of thymidylate synthase-catalyzed reaction and interaction of the enzyme with 2- and/or 4-substituted analogues of dUMP and 5-fluoro-dUMP. *Acta Biochim Pol* 43:133–142.
4. Barrett J, Maltby D, Santi D, Schultz P (1998) Trapping of the C5 methylene intermediate in thymidylate synthase. *J Am Chem Soc* 120:449–450.
5. Phan J, et al. (2000) Catalytic cysteine of thymidylate synthase is activated upon substrate binding. *Biochemistry* 39:6969–6978.
6. Kanaan N, Martí S, Moliner V, Kohen A (2007) A quantum mechanics/molecular mechanics study of the catalytic mechanism of the thymidylate synthase. *Biochemistry* 46:3704–3713.
7. Kaiyawet N, Lonsdale R, Rungrotmongkol T, Mulholland AJ, Hannongbua S (2015) High-level QM/MM calculations support the concerted mechanism for Michael addition and covalent complex formation in thymidylate synthase. *J Chem Theory Comput* 11:713–722.
8. Wang Z, Ferrer S, Moliner V, Kohen A (2013) QM/MM calculations suggest a novel intermediate following the proton abstraction catalyzed by thymidylate synthase. *Biochemistry* 52:2348–2358.
9. Islam Z, Strutzenberg TS, Gurevic I, Kohen A (2014) Concerted versus stepwise mechanism in thymidylate synthase. *J Am Chem Soc* 136:9850–9853.
10. Moore MA, Ahmed F, Dunlap RB (1986) Trapping and partial characterization of an adduct postulated to be the covalent catalytic ternary complex of thymidylate synthase. *Biochemistry* 25:3311–3317.
11. Huang W, Santi DV (1994) Isolation of a covalent steady-state intermediate in glutamate 60 mutants of thymidylate synthase. *J Biol Chem* 269:31327–31329.
12. Doan LT, Martucci WE, Vargo MA, Atreya CE, Anderson KS (2007) Nonconserved residues Ala287 and Ser290 of the Cryptosporidium hominis thymidylate synthase domain facilitate its rapid rate of catalysis. *Biochemistry* 46:8379–8391.
13. Johnson EF, Hinz W, Atreya CE, Maley F, Anderson KS (2002) Mechanistic characterization of Toxoplasma gondii thymidylate synthase (TS-DHFR)-dihydrofolate reductase. Evidence for a TS intermediate and TS half-sites reactivity. *J Biol Chem* 277:43126–43136.
14. Atreya CE, Anderson KS (2004) Kinetic characterization of bifunctional thymidylate synthase-dihydrofolate reductase (TS-DHFR) from Cryptosporidium hominis: A paradigm shift for ts activity and channeling behavior. *J Biol Chem* 279:18314–18322.
15. Kholodar SA, Kohen A (2016) Noncovalent intermediate of thymidylate synthase: Fact or fiction? *J Am Chem Soc* 138:8056–8059.
16. Hardy LW, Nalivaika E (1992) Asn177 in Escherichia coli thymidylate synthase is a major determinant of pyrimidine specificity. *Proc Natl Acad Sci USA* 89:9725–9729.
17. Hardy LW (1995) Structural aspects of the inhibition and catalytic mechanism of thymidylate synthase. *Acta Biochim Pol* 42:367–380.